Med Biol Eng Comput (2011) 49:1289–1297
DOI 10.1007/s11517-011-0834-z

ORIGINAL ARTICLE

Asymmetric properties of long-term and total heart rate variability

Jaroslaw Piskorski · Przemyslaw Guzik

Received: 3 March 2011 / Accepted: 8 September 2011 / Published online: 28 September 2011

Abstract We report on two new physiological phenomena: the long-term and total heart rate asymmetry, which describe a significantly larger contribution of heart rate accelerations to long-term and total heart rate variability. In addition to the existing pair of indices, $SD1_d, SD1_a$, which are based on partitioning short-term variance, we introduce two other pairs of descriptors based on partitioning long-term ($SD2_d, SD2_a$) and total ($SDNN_d, SDNN_a$) heart rate variability. The new asymmetric descriptors are used to analyze RR intervals time series derived from the 30-min ECG recordings of 241 healthy subjects resting in supine position. It is shown that both new types of asymmetry are present in 76% of the subjects. The new phenomena reported here are real physiological findings rather than artifacts of the method since they vanish after data shuffling.

Keywords Heart rate variability · Heart rate asymmetry · Poincaré plot

1 Introduction

Variation in the beat-to-beat duration of cardiac cycles or *RR* intervals, i.e., the distances between consecutive peaks of R waves of QRS complexes in an ECG signal, is termed heart rate variability (HRV) [1, 34]. This variation is influenced by various physiological mechanisms, most of which are mediated by the sympathetic and parasympathetic branches of the autonomic nervous system. It was first assumed and later proved that HRV measures can be used as indices of autonomic activity or sympathetic–parasympathetic balance [1, 34].

Apart from reflecting a number of physiological features [1, 7, 17, 34], HRV has been shown to change in different clinical settings like in patients with arterial hypertension, heart failure, diabetes mellitus, after cardiac transplantation or in survivors of sudden cardiac death [1, 11, 15, 21, 34]. One of the most interesting and important properties of HRV is its predictive value in cardiac patients—reduced HRV is associated with increased mortality risk in patients after myocardial infarction or with advanced heart failure [1, 3, 4, 34].

Numerous methods and descriptors are applied to quantify HRV [1, 34]. The short- and long-term components have been identified in the total HRV [1, 5, 12, 34]. It is accepted that high frequency oscillations are responsible for the short-term HRV, whereas long-term HRV is mainly generated by low frequency oscillations [1, 34].

The absolute values of changes in RR intervals, irrespective of their true direction (shortening or prolongation of RR intervals), have been taken into consideration in HRV analysis for many years. Recently, some new methods of HRV analysis separating the information derived from heart rate accelerations and decelerations have been proposed [3, 6, 10, 14, 16, 19, 27, 29, 30]. The application of Poincaré plots of RR intervals enabled the discovery of a new physiological phenomenon of heart rate asymmetry (HRA) [10, 27].

HRA is a physiological phenomenon reflecting the consistently different contribution of heart rate decelerations and accelerations to a variance-based descriptors of

J. Piskorski (✉)
Institute of Physics, University of Zielona Gora, Szafrana 4a, Zielona Gora, Poland
e-mail: jaropis@zg.home.pl

P. Guzik
Department of Cardiology-Intensive Therapy and Internal Diseases, Poznan University of Medical Sciences, Przybyszewskiego 49, Poznan, Poland

the variability of RR intervals time series. So far, it has been defined with respect to the short-term variance: the contribution to short-term variance ($SD1^2$) from decelerations is consistently and highly statistically significantly greater than that from accelerations. The partitioning of $SD1^2$ defines two HRA descriptors, namely $SD1_d$ and $SD1_a$ (a for accelerations and d for decelerations), whose sum of squares equals $SD1^2$ i.e., the short-term variability. This partitioning is physiologically interpretable [27]. In this article, we define two new pairs of variance-based HRA descriptors—this time for long-term variance ($SD2^2$) and total variance ($SDNN^2$). Our objective is to check, with the use of the above descriptors, whether there is a consistent and one-directional asymmetry in the long-term and total variability.

2 Methods

HRA can be best understood with the use of the Poincaré plot, so we begin with a short introduction to this approach, after which the HRA descriptors are introduced and interpreted.

Let

$$\mathbf{RR_n} \equiv (\mathrm{RR}_1, \mathrm{RR}_2, \ldots, \mathrm{RR}_n), \tag{1}$$

be a time series of RR intervals indexed by the heart-beat number. The Poincaré plot is a visual representation of the RR intervals time series in a plane. Each point has coordinates $(\mathrm{RR}_i, \mathrm{RR}_{i+1})$, so that it binds an RR interval with the next one. The standard descriptors of the Poincaré plot, are SDNN, reflecting the total variability, and SD1, SD2 which are widely believed to reflect short- and long-term HRV, respectively [5]. In Fig. 1, we show the standard descriptors as well as SDNN and other characteristics of the Poincaré plot like the identity line, l_1 and l_2 centroid lines and the centroid itself.

The construction of the Poincaré plot leads to a clear division into the points above and below the identity line, which correspond to heart rate decelerations and accelerations, respectively.

For completeness, let us quote the formulas for the standard Poincaré plot descriptors [5, 27]

$$\mathrm{SD1}^2 = \mathrm{Var}\left(\frac{\mathbf{RR_{n+1}} - \mathbf{RR_n}}{\sqrt{2}}\right), \tag{2}$$

$$\mathrm{SD2}^2 = \mathrm{Var}\left(\frac{\mathbf{RR_{n+1}} + \mathbf{RR_n}}{\sqrt{2}}\right), \tag{3}$$

where

$$\mathbf{RR_n} \equiv \{\mathrm{RR}_1, \mathrm{RR}_2, \ldots, \mathrm{RR}_n\}, \tag{4}$$

$$\mathbf{RR_{n+1}} \equiv \{\mathrm{RR}_2, \mathrm{RR}_3, \ldots, \mathrm{RR}_{n+1}\},$$

and finally

$$\mathrm{SDNN}^2 = \frac{1}{2}(\mathrm{SD1}^2 + \mathrm{SD2}^2). \tag{5}$$

In [27], we slightly redefined the $SD1^2$ descriptor basing it on the line of identity rather than on the centroid line, so, we have defined

$$\mathrm{SD1}_I^2 \equiv \frac{1}{n}\sum_{i=1}^{n}[r^{\perp}]_i^2, \tag{6}$$

where $r_i^{\perp}$ is the perpendicular distance from a Poincaré plot point to the line of identity. Since $SD1^2$ is the variance and $SD1_I^2$ is another second moment of the points distribution, we have

$$\Delta = \mathrm{SD1}_I^2 - \mathrm{SD1}^2 \geq 0. \tag{7}$$

The magnitude of Δ is so small, especially for longer recordings, that we can assume that both these moments are practically equal. A more thorough discussion can be found in [27].

The HRA phenomenon demonstrates one way in which the heart rate deceleration process quantitatively and qualitatively differs from the acceleration process. In previous articles we showed this phenomenon at the short-time scale. To do this, we partitioned the short-term variance, i.e., $SD1_I^2$ into parts corresponding to accelerations and decelerations separately [10, 12, 27]. Below we briefly describe the concept of short-term asymmetry, introduce long-term asymmetry Poincaré plot descriptors and partition the full Poincaré plot variance ($SDNN^2$) into asymmetric parts based on accelerations and decelerations of heart rhythm.

2.1 Short-term HRA descriptors

Following the methodology of [27], we will partition the second moment of the Poincaré plot cloud with respect to the line of identity. Assuming the following nomenclature: $r_i^{\perp\,\mathrm{d}}$—perpendicular distance from the decelerating Poincaré plot point number i to the line of identity, $r_j^{\perp\,\mathrm{a}}$—perpendicular distance from the accelerating Poincaré plot point number j to the line of identity, we can partition the short-term variability $SD1^2$ (6) in the following way

$$\mathrm{SD1}^2 = \frac{1}{n}\left(\sum_{i=1}^{n_\mathrm{d}}[r_i^{\perp\,\mathrm{d}}]^2 + \sum_{j=1}^{n_\mathrm{a}}[r_j^{\perp\,\mathrm{a}}]^2\right), \tag{8}$$

where n_d is the number of decelerations (points above the identity line), n_a is the number of accelerations (points below the identity line). For completeness, we also define n_on as the number of points on the identity line (points which correspond to no change in heart rate between two

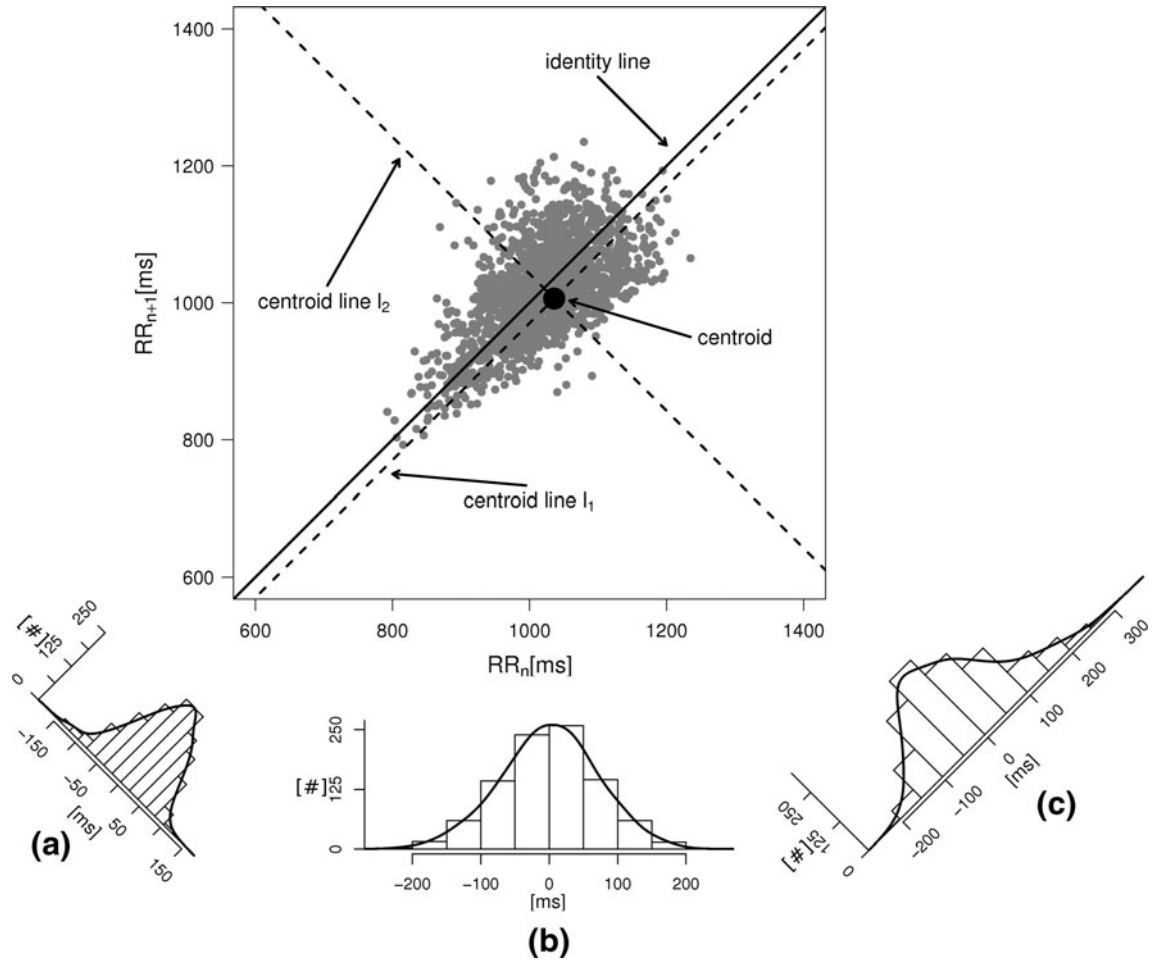

Fig. 1 An example Poincaré plot of RR intervals derived from a 30-min ECG recording taken from a 28-year-old healthy male at rest. The identity line divides the Poincaré plot into two areas—decelerations are located above and accelerations below this line. Two centroid lines are also shown: both pass through the centroid, l_1 is parallel to the identity line, l_2 is perpendicular. The position of the centroid is exaggerated for clearness. As described in [5], the variance of the projection of the Poincaré plot points along the identity line is the short-term variability $SD1^2$ (histogram **a**), perpendicular projection leads to long-term variance $SD2^2$ (histogram c) and the variance of the projection on RR_n is $SDNN^2$. The figure is based on [5] and [27]

consecutive heart beats), and which do not contribute to the short-term variability, to get

$$n = n_{\mathrm{d}} + n_{\mathrm{a}} + n_{\mathrm{on}}. \tag{9}$$

This partitioning lets us naturally define descriptors corresponding to contributions to $SD1^2$ from accelerations and decelerations separately

$$\mathrm{SD1}^2 = \mathrm{SD1}_{\mathrm{d}}^2 + \mathrm{SD1}_{\mathrm{a}}^2, \tag{10}$$

with

$$\mathrm{SD1}_{\mathrm{d}}^2 = \frac{1}{n}\sum_{i=1}^{n_{\mathrm{d}}}[r_i^{\perp \mathrm{d}}]^2, \qquad \mathrm{SD1}_{\mathrm{a}}^2 = \frac{1}{n}\sum_{i=1}^{n_{\mathrm{a}}}[r_i^{\perp \mathrm{a}}]^2. \tag{11}$$

Using the above we define normalized contributions of decelerations and accelerations to $SD1^2$ as

$$C1_{\mathrm{d}} = \frac{\mathrm{SD1}_{\mathrm{d}}^2}{\mathrm{SD1}^2}, \qquad C1_{\mathrm{a}} = \frac{\mathrm{SD1}_{\mathrm{a}}^2}{\mathrm{SD1}^2}, \tag{12}$$

with

$$C1_{\mathrm{d}} + C1_{\mathrm{a}} = 1. \tag{13}$$

The above process is illustrated by a of Fig. 2.

In [27], we defined HRA as a situation where in a group of N subjects we have

$$C1_d > C1_{\mathrm{a}}, \tag{14}$$

and this effect is statistically significant.

In [27], it was shown that short-term heart asymmetry is present in RR intervals time series recordings from healthy resting subjects.

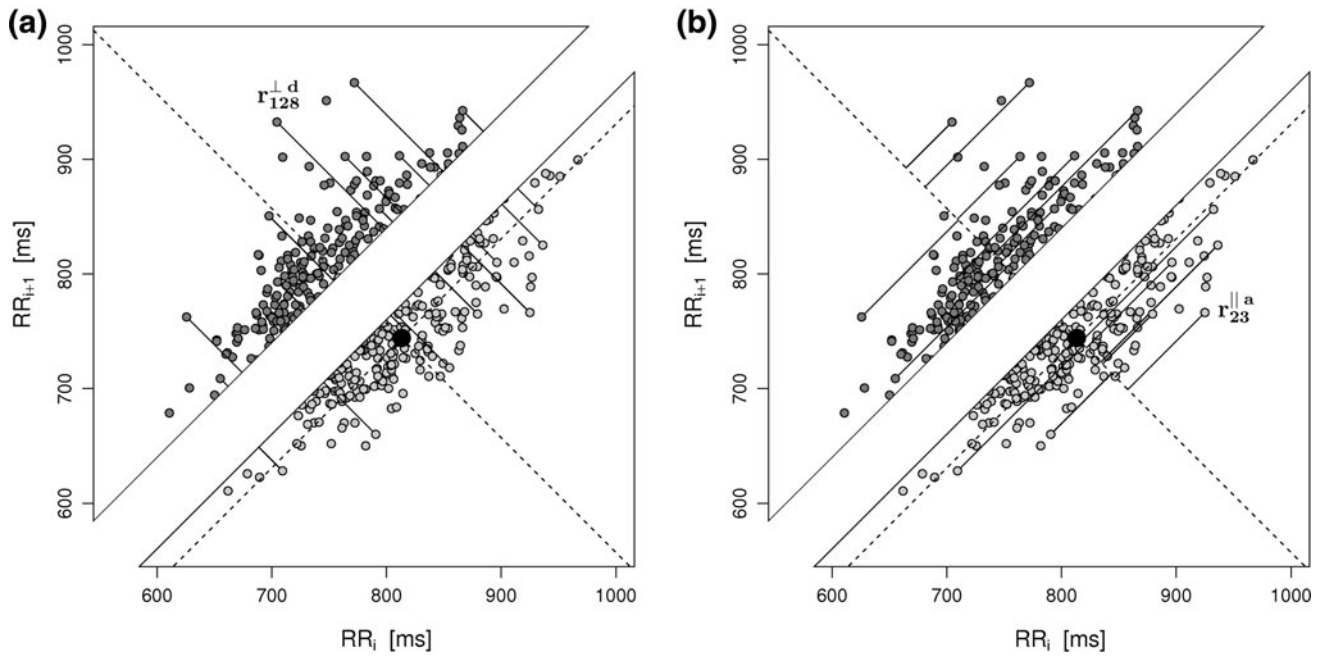

Fig. 2 In **a**, the process of calculating the short-term HRA is presented, **b** shows long-term HRA. Note that the identity line is the most important geometric object in both procedures—it is the main criterion for deciding whether a point contributes to the decelerations or accelerations related part of the specific variances ($SD1^2$ or $SD2^2$). For some points the perpendicular distances $r_i^{\perp \mathrm{d}}$ to the identity line (compare formula 6) are drawn in **a** and $r_i^{\| \mathrm{a}}$ (compare formula 15) to l_2 in **b**. For clarity most points are not connected, but the distances are calculated for all of them. For two points the segments are explicitly marked, namely for Poincaré plot point number 128 (a decelerating point) in **a** and 23 (an accelerating point) in **b**

2.2 Partitioning of $SD2^2$

In this subsection we define, for the first time, long-term variability ($SD2^2$) partitioning. The meaning of long-term in this article refers to the construction of the parameter and can be calculated for recordings of any length. This is similar to the usage of terms "high frequency", "low frequency", and "very low frequency" in spectral techniques—they can be calculated for recordings of many different lengths, provided that they are stationary and are long enough to have the calculated component. The arguments for considering $SD2^2$ as a long-term parameter are given in [5]. However, in this article the time-scale for studying long-term variability is 30 min. For this reason, the conclusions drawn here refer to this time-scale.

$SD2^2$ is the second moment of the Poincaré plot around the centroid l_2 line [27]. Since this is the lowest possible moment, it can be called the long-term variance. As explained in [27], the line of identity is the only physiologically interpretable line in Fig. 1, l_1 and l_2 lines being geometrical objects describing only the distribution of points in a specific Poincaré plot . Hence, for partitioning $SD2^2$ we will still use the line of identity rather than l_2, even though the second moment is calculated around l_2. The choice of l_2 is based on two properties of variance—first, it will give us an exact partitioning of $SD2^2$, second, it is the smallest possible second moment in this direction.

Let us assume the following nomenclature: $r_i^{\| \mathrm{d}}$ —distance along the line of identity from the decelerating Poincaré plot point number i to l_2, $r_j^{\| \mathrm{a}}$ –distance along the line of identity from the accelerating Poincaré plot point number j to l_2.

For the finite resolution measurement, we partition $SD2^2$ noticing that some points will be located exactly on the identity line. Therefore

$$\begin{aligned} SD2^2 &= \frac{1}{n}\sum_{k=1}^{N} r_k^{\| 2} \\ &= \frac{1}{n}\left(\sum_{i=1}^{n_{\mathrm{d}}}[r_i^{\| \mathrm{d}}]^2 + \sum_{j=1}^{n_{\mathrm{a}}}[r_j^{\| \mathrm{a}}]^2 + \sum_{k=1}^{n_{\mathrm{on}}}[r_k^{\| \mathrm{on}}]^2\right), \end{aligned} \tag{15}$$

where $r_k^{\|}$ stands for the distance of point k along the line of identity to l_2 and $n_{\mathrm{d}}, n_{\mathrm{a}}, n_{\mathrm{on}}$ are defined as above.

The first two components of the right side of Eq. 15 can be easily identified as the contributions to $SD2^2$ only from decelerating points (first sum) and accelerating points (second sum).

The qualitative difference between Eqs. 10,11 and 15 is the presence of the $1/n\sum_{j=1}^{n_{\mathrm{on}}}[r_j^{\| \mathrm{on}}]^2$ part in (15). The points

located directly on the line of identity do not contribute to $SD1^2$ (compare Sect. 2.1), because their distance to the identity line is exactly 0. However, they do contribute to $SD2^2$, as their distance to l_2 is non-zero.

The size of the $1/n \sum_{j=1}^{n_{on}} [r_j^{||\,on}]^2$ part depends on the resolution of the measuring equipment—the lower the resolution, the more the overall degeneracy of the measurement and, consequently, the more points lie on the identity line. Contrariwise, if we imagine a perfect measurement with resolution tending to infinity, the probability that two consecutive points of the RR intervals time series are equal would tend to zero, and so would the above contribution to variance.

There are a few possible ways to address the presence of this identity line generated part of variance. We suggest this part be equally distributed between parts corresponding to decelerations and accelerations—in this way, the statistical tests will be more conservative. Thus, we define the following partitioning of $SD2^2$ between accelerations and decelerations

$$SD2^2 = SD2_d^2 + SD2_a^2, \tag{16}$$

which has the same form as (10), but where the respective parts are defined as

$$\begin{aligned} SD2_d^2 &= \frac{1}{n}\left(\sum_{i=1}^{n_d}[r_i^{||\,d}]^2 + \frac{1}{2}\sum_{j=1}^{n_{on}}[r_j^{||\,on}]^2\right), \\ SD2_a^2 &= \frac{1}{n}\left(\sum_{i=1}^{n_a}[r_i^{||\,a}]^2 + \frac{1}{2}\sum_{j=1}^{n_{on}}[r_j^{||\,on}]^2\right). \end{aligned} \tag{17}$$

Just like in Eq. 12, we can define normalized contributions from decelerations and accelerations to $SD2^2$ as

$$C2_d = \frac{SD2_d^2}{SD2^2}, \qquad C2_a = \frac{SD2_a^2}{SD2^2}, \tag{18}$$

where

$$C2_d + C2_a = 1. \tag{19}$$

This partitioning process and its various steps are illustrated by b of Fig. 2.

2.3 $SDNN^2$ partitioning

Using Eqs. 5,10,16, we can formally partition the total variability ($SDNN^2$) in the following way

$$\begin{aligned} SDNN^2 &= \frac{1}{2}\left(\underbrace{(SD1_d^2 + SD1_a^2)}_{SD1^2} + \underbrace{(SD2_d^2 + SD2_a^2)}_{SD2^2}\right) \\ &= \frac{1}{2}\left(\underbrace{(SD1_d^2 + SD2_d^2)}_{2SDNN_d^2} + \underbrace{(SD1_a^2 + SD2_a^2)}_{2SDNN_a^2}\right). \end{aligned} \tag{20}$$

Thus, we define

$$SDNN^2 = SDNN_d^2 + SDNN_a^2, \tag{21}$$

with

$$\begin{aligned} SDNN_d^2 &= \frac{1}{2}\left(SD1_d^2 + SD2_d^2\right), \\ SDNN_a^2 &= \frac{1}{2}\left(SD1_a^2 + SD2_a^2\right). \end{aligned} \tag{22}$$

Partitioning (22) leads to the following formula for the contributions of accelerations and decelerations to total variability:

$$C_d + C_a = 1, \tag{23}$$

where

$$C_d \equiv \frac{SDNN_d^2}{SDNN^2}, \qquad C_a \equiv \frac{SDNN_a^2}{SDNN^2}. \tag{24}$$

Above we have introduced two new sets of partitioning-based descriptors based on long-term variance and total variance. Any systematic departure from the equality of $C2_d$ and $C2_a$ as well as C_d and C_a would constitute long-term and total HRA phenomena. This will be tested in the next section.

At this point it is worth mentioning that our approach to HRA is one-directional. There are other approaches which are not one-directional [19] and we believe that these approaches refer to different properties of heart rhythm variability than ours. In the next subsection, we attempt to address this problem.

2.4 The directionality of HRA

In this article, as well as in all the previous ones we have stressed that our definition of asymmetry is one-directional, that is one of the asymmetry descriptors has to be consistently bigger/smaller for us to be able to declare that there is asymmetry. Other approaches which accept asymmetry whenever the conjugated asymmetry descriptors are *different* can also be considered. With these approaches it is easier to establish asymmetry, however, we believe that they have weaker mathematical justification. These types of asymmetry may not correspond to any physiological phenomena—they may just be an artifact of the method. They are also more difficult to interpret physiologically.

In a Poincaré plot, there are at least two components driving its geometry: the physiology and stochasticity. If the two-directional asymmetry definition mentioned above is accepted, the stochastic component will almost certainly generate asymmetry even for a perfectly symmetric process, since a totally balanced plot (perfectly equal on both sides of the identity line) is actually rare, which can be shown on the basis of probability analysis.

Let us draw an analogy. Let us assume that in an RR intervals time series the probability of the next interval being an acceleration or deceleration is purely random and that the probability of either result is the same. This situation is equivalent to the classic fair coin-tossing experiment, with probability $P = 1/2$ for both heads and tails. Let us now toss the coin 100 times—this will be a single "Poincaré plot " consisting of 100 points. The probability that in this experiment we will get exactly 50 heads is

$$P(\text{symmetry}) = \binom{100}{50}(1/2)^{100} \simeq 0.08, \quad (25)$$

while all the other "asymmetric" results will have the joint probability of

$$P(\text{asymmetry}) \simeq 1 - 0.08 = 0.92. \quad (26)$$

This means that in a sample of 100 recordings generated in the above described way, in the bidirectional approach, 92% "asymmetric" Poincaré plots are expected and they do *not* prove any kind of asymmetry in the analyzed process. A perfectly symmetric process such as this *must* have 92% "asymmetric" Poincaré plots.

To alleviate this problem a "safety" region can be selected—in [19] it is ±1% of the difference between the minimum and maximum of the studied asymmetry index value. Still, this type of asymmetry may mainly be driven by the stochastic component, and there is the problem of the arbitrary width of the "safety" region. The statistical test can only be designed if the region is judiciously selected—this is possible, but unwieldy. Also, the interpretation of such an asymmetry is more difficult: in our approach, we attribute certain parts of variance to heart rate decelerations or accelerations. If the two-directional approach is assumed, it can no longer define its parameters separately for decelerations and accelerations. The one-directional approach seems mathematically better justified, leads to a well defined statistical test, and is physiologically more easily interpretable.

2.5 Statistical analysis

For the analysis, we use the binomial test for comparing the numbers of asymmetric cases and the Wilcoxon test for comparing the relative contributions. Our zero hypothesis (H_0) is that there is no asymmetry. We will conclude the presence of asymmetry if (a) a significant number of subjects shows asymmetry of the same direction and (b) if the contribution either from decelerations or accelerations are consistently and significantly greater. The motivation for using these statistical techniques as well as the sample size calculation may be found in [27].

To check whether the obtained results reflected the physiological structure of the time series rather than being just an artifact of the method, we used the shuffled-data approach based on a random number generator. From the mathematical construction of the descriptors it follows that after shuffling no asymmetry should be observable.

2.6 Materials

30-min long RR intervals time series were analyzed. For this study, 241 young, healthy volunteers were enrolled (22–25 years of age, 105 women). All subjects refrained from smoking, alcohol, and coffee for 24 h before the study. No participant was addicted to drugs, taking any medications, or involved in endurance training. All volunteers gave informed consent to participate in the study. This project was approved by the Poznan University of Medical Science Bioethics Committee.

2.7 Protocol

The study was performed at rest in the supine position, and the subjects were kept quiet in a neutral environment. The subjects were allowed to breathe spontaneously during the whole study. The 30-min recording was taken after a preceding 15-min period used for cardiovascular adaptation. Three channels of a bipolar chest lead ECG were recorded with a sampling frequency of 1600 Hz by an A/D converter (Porti 5, TMSI, The Netherlands). The data were transferred on-line to a PC for on-screen monitoring and data storage. The preliminary automatic evaluation of the recordings was performed with the use of the libRASCH/RASCHlab software from the libRASCH project (v. 0.6.1; http://www.librasch.org, Germany). This was followed by visual inspection of all signals and necessary corrections of the obtained values [32], i.e., beats misclassified by the software were corrected. The values of the RR intervals were retrieved from the stored recordings and used in further analysis. The data were analyzed with the use of in-house software written in Python (Python Foundation, USA). The statistical analysis was performed with the use of the R statistical package (R-project, http://www.r-project.org). The RR intervals time series were filtered as described in [26] to correctly remove all points involving ectopic beats and artifacts.

3 Results

3.1 Short-term asymmetry

$SD1_d > SD1_a$ was observed in 199 subjects which is 82.6% of the group. This is a highly statistically significant result in the binomial test, $P < 0.0001$. The mean $C1_d$ was 0.54; the Wilcoxon test yields a highly significant results

with $P < 0.0001$. Short-term HRA is clearly present in the studied group.

After shuffling both effects disappeared—approximately half (121) shuffled recordings had $SD1_d > SD1_a$ and $C1_d$ was close to 0.5 (0.495)—*P*-value not significant in both tests.

3.1.1 Long-term asymmetry

$SD2_d < SD2_a$ was observed in 184 subjects which is 76.4% of the group. This is a highly statistically significant result in the binomial test, $P < 0.0001$. The mean $C2_d$ was 0.47; the Wilcoxon test yields a highly significant result with $P < 0.0001$.

We note that there is a consistent effect with $SD2_a > SD2_d$. The criterion for establishing the presence of asymmetry defined in [27], that is the requirement that one-directional asymmetry is observable in at least 70% cases is fulfilled. Therefore, we can report on a *new HRA phenomenon*, namely the *long-term HRA*. Note that for long-term asymmetry it is the *accelerations* that have a greater contribution than decelerations to long-term variability.

After shuffling the effects disappeared—approximately half (127) shuffled recordings had $SD2_d < SD1_a$ and $C2_a$ was close to 0.5 (0.499)—*p*-value not significant in both tests.

3.1.2 Total asymmetry

$SDNN_d < SDNN_a$ was observed in 184 (exactly the same number as above) subjects which is 76.4% of the group. This is a highly statistically significant result in the binomial test, $P < 0.0001$. The mean C_d was 0.48; the Wilcoxon test yields a highly significant result with $P < 0.0001$

We note that there is a consistent effect with $SDNN_a > SDNN_d$. As with the long-term asymmetry, all the statistical conditions for establishing asymmetry were met, so we can report on another HRA phenomenon, namely the *total HRA*.

After shuffling the effects disappeared—approximately half (127) shuffled recordings had $SDNN_d < SDNN_a$ and C_a was close to 0.5 (0.496)—*P*-value not significant in both tests.

3.2 HRA emergence

As it was mentioned, the maximum time scale of the present analysis is 30 min. In [10], the short-term asymmetry was observed in stationary recordings of 5 min. Therefore, it is interesting to check what the prevalence of all types HRA is for shorter recordings.

To answer this question we cut the recordings into two (15 min) and three (10 min) parts and used the first segment of each recording. The result for 15 min segments are the following: short-term HRA is observed in 75% of the studied subjects, long-term HRA in 70%, and total HRA in 68%. In 10 min recordings, short-term HRA was present in 73%, long-term HRA in 66%, and total HRA in 65%. All these results are statistically significant with $P < 0.001$.

We have also checked much shorter segments. Since the sample size is 241, the smallest proportion in the binomial test that significantly differs from 0.5 is 0.57 (with $P = 0.039$). This proportion is reached after as short a time as 1 min for all three types of asymmetry (0.57 for short-term, 0.58 for long-term and total asymmetry). Therefore, in this study, HRA can be observed after just 1 min of stationary ECG recording. The analysis of this subsection is based on [20, 23–25].

4 Discussion

In this article, we have described two new phenomena which can be observed in resting patients in supine position, namely the long-term and total HRA. The long-term asymmetry complements the already known short-term asymmetry, and the total HRA is a net result of these two phenomena. The long-term asymmetry is the statistically significantly lower contribution of heart rate decelerations to the long-term variability, namely $SD2^2$. This effect is opposite to what is observed in the short-term HRA, in which decelerations have a significantly larger contribution to short-term variability, i.e., $SD1^2$. The formal partitioning of total HRV into a part contributed by accelerations and a part contributed by decelerations leads to the second observation reported in this article, namely total HRA in which decelerations have a lower contribution than accelerations. Clearly, in total HRA, long-term asymmetry prevails.

Another important finding of our physiological study is that heart rate decelerations and accelerations influence the short-term HRV differently than the long-term or total HRV. A possible explanation for this is *compensation* within HRA. The more dynamic decelerations, contributing more to short-term variability are compensated for by less dynamic accelerations, which have to act on a longer time-scale to balance out the decelerations (compare [28]). Whether this compensation is an effect of antagonistic and compensatory function of the sympathetic and parasympathetic systems or some cardiovascular reflexes with negative feedback (e.g., baroreflex), remains a speculation only.

All types of asymmetry are abolished after data shuffling. In this article, we have used the shuffling randomization method with the use of a random number generator, however, any randomization scheme which destroys the phasic information must yield the same result.

The underlying mathematical representation of the phenomena reported could lie in the different structure of runs of decelerations and accelerations described in [28]. The analyzes of [2, 18] in which fluctuations of magnitudes and signs of the RR increments were analyzed and different behaviors of these two were found at various time-scales could also shed some light on the results reported here.

Various physiological mechanisms could be responsible for HRA. HRA is a part of HRV which is related to and used for the evaluation of the autonomic modulation of the cardiovascular system. For example, baroreflex exhibits some asymmetry, as baroreflex sensitivity is different for blood pressure increases and reductions, even for the same magnitude of blood pressure absolute changes [22, 31]. For this reason, we are inclined to assume that HRA is under some influence of the autonomic nervous system, particularly baroreflex. Another plausible mechanism might be more mechanical. Respiratory sinus arrhythmia is a physiological phenomenon by which the duration of cardiac cycles during a single breath varies—the RR intervals shorten during inspiration and increase during expiration [1, 8, 9, 34]. Usually, the duration of inspiration and expiration is not equal, i.e., it is asymmetrical, and this respiratory sinus arrhythmia is also responsible for different amount of blood getting in and being ejected from both ventricles of the heart throughout each breathing cycle. Some other mechanisms can also be considered with a number of factors regulating the duration of each cardiac cycle, like changes in the action potential caused by the changes in potassium and sodium concentration in the natural pacemaker (sinus node) as well as variations in acetylocholine, norepinephrine, or other neurotransmitters regulating the momentary heart rate [33, 34]. It is also possible that HRA is generated by a combination of all or some of the mechanisms mentioned above or by another mechanism, which is not listed here.

Only a few physiological and clinical studies have evaluated HRA so far. Porta et. al.have shown that HRA changes during head-up tilting in healthy people. In the same paper they showed that HRA changes in fetuses between 16th to 40th week of gestation [29]. Porta et. al. [30] have reported that the relative number of heart rate decelerations during a day is significantly reduced in patients with chronic heart failure compared with control subjects. Our group has shown that measures of HRA are reduced in patients with type 1 diabetes of a very long duration (at least 25 years) both in resting 10-min ECGs and in 24-h ambulatory ECGs compared to healthy age-matched controls [11]. In addition, we have reported that the measures of the structure of HRA, i.e., deceleration runs, are reduced in post-infarction patients with increased risk of mortality during a 2-year follow-up [14].

All these studies clearly show that HRA is not only some peculiarity and a newer approach to HRV but it carries physiological and clinical information.

It appears that asymmetrical properties can be found not only in HRV but also in the blood pressure variability as increases in systolic blood pressure have significantly larger contribution to short-term blood pressure variability than reductions. HRA and blood pressure variability asymmetry are independent phenomena [13].

HRA is a new and poorly understood phenomenon. It has a clear presence in healthy resting subjects and the methods to quantify it are quite straightforward and interpretable, so it should be simple to study it in more detail and in different clinical settings by other researchers. More methodological, exploratory, explanatory and practical studies are needed to better understand HRA.

To conclude, in this article, we have reported on new, so far unknown aspects of HRA, namely that the contributions of accelerations to long-term and total HRV are significantly greater than those of accelerations. These effects are opposite to the effect found earlier in short-term HRV. To study these aspects of HRV, we have introduced a new way of partitioning variance associated with RR intervals time series.

Acknowledgments This study is a part of the project "Predicting adverse clinical outcomes in patients with implanted defibrillating devices", which is supported by the Foundation for Polish Science - TEAM program co-financed by the European Union within the European Regional Development Fund.

References

1. Acharya UR, Joseph KP, Kannathal N, Lim CM, Suri JS (2006) Heart rate variability: a review. Med Biol Eng Comput 44: 1031–51
2. Ashkenazy Y, Havlin S, Ivanov PC, Peng CK, Schulte-Frohlinde V, Stanley HE (2003) Magnitude and sign scaling in power-law correlated time series. Physica A 323:19-41
3. Bauer A, Kantelhardt JW, Barthel P, Müller A, Ulm K, Hnatkova K, Schöming A, Huikuri H, Bunde A, Malik M, Schmidt G (2006) Deceleration capacity of heart rate as a predictor of mortality after myocardial infarction: cohort study. Lancet 367: 1674–1681
4. Bauer A, Barthel P, Schneider R, Ulm K, Müller A, Joeinig A, Stich R, Kiviniemi A, Hnatkova K, Huikuri H, Schömig, Malik M, Schmidt G (2009) Improved Stratification of Autonomic Regulation for risk prediction in post-infarction patients with

preserved left ventricular function (ISAR-Risk). Eur Heart J 30:576-583
5. Brennan M, Palaniswami M, Kamen P (2001) Do existing measures of Poincar plot geometry reflect nonlinear features of heart rate variability?. Trans Biomed Eng 48:1342–1347
6. Cassali KR, Cassali AG, Montano N, Irigoyen MC, Macagnan F, Guzzetti S, Porta A (2008) Multiple testing strategy for the detection of temporal irreversibility in stationary time series. Phys Rev E 77:006204
7. Castiglioni P, Di Rienzo M, Veicsteinas A, Parati G, Merati G (2007) Mechanisms of blood pressure and heart rate variability: an insight from low-level paraplegia. Am J Physiol Regul Integr Comp Physiol 292:R1502–R1509
8. Eckberg DL (1983) Human sinus arrhythmia as an index of vagal cardiac outflow. J Appl Physiol 54:961–966
9. Eckberg DL (2003) The human respiratory gate. J Physiol 548:339–52
10. Guzik P, Piskorski J, Krauze T, Wykretowicz A, Wysocki H (2006) Heart rate asymmetry by Poincaré plots of RR intervals. Biomed Tech (Berl) 51:272–275
11. Guzik P, Piskorski J, Contreras P, Migliaro ER (2010) Asymmetrical properties of heart rate variability in type 1 diabetes. Clin Auton Res 20:255–257
12. Guzik P, Piskorski J, Krauze T, Wykretowicz A, Wysocki H (2010) Partitioning total heart rate variability. Int J Cardiol 144:138–139
13. Guzik P, Piskorski J, Wykretowicz A, Wysocki H, Narkiewicz K (2010) Asymmetric features of short-term blood pressure variability. Hypertens Res 33:1199–1205
14. Guzik P, Piskorski J, Barthel P, Bauer A, Müller A, Junk N, Ulm K, Malik M, Schmidt G (2011) Heart rate deceleration runs for post-infarction risk prediction. J Electrocardiol. doi:10.1016/j.jelectrocard.2011.08.006
15. Heitmann A, Huebner T, Schroeder R, Perz S, Voss A (2011) Multivariate short-term heart rate variability: a pre-diagnostic tool for screening heart disease. Med Biol Eng Comput 49:41–50
16. Houa F, Zhuanga J, Biana C, Tonga T, Chena Y, Yina J, Qiuc X, Ninga X (2010) Analysis of heartbeat asymmetry based on multiscale time irreversibility test. Physica A 389:754–760
17. Jo JA, Blasi A, Valladares E, Juarez R, Baydur A, Khoo MC (2005) Determinants of heart rate variability in obstructive sleep apnea syndrome during wakefulness and sleep. Am J Physiol Heart Circ Physiol 288:H1103–H1112
18. Kantelhardt JW, Ashkenazy Y, Ivanov PC, Bunde A, Havlin S, Penzel T, Peter JH, Stanley HE (2001) Characterization of sleep stages by correlations in the magnitude and sign of heartbeat increments. Phys Rev E 65:051908
19. Karmakar CK, Khandoker AH, Gubbi J, Palaniswami M (2009) Defining asymmetry in heart rate variability signals using a Poincaré plot. Physiol Meas 30:1227–1240
20. Kobayashi M, Musha T (1982) 1/f fluctuation of heartbeat period. IEEE Trans Biomed Eng 29:456–457
21. Melillo P, Fusco R, Sansone M, Bracale M, Pecchia L (2011) Discrimination power of long-term heart rate variability measures for chronic heart failure detection. Med Biol Eng Comput 49:67–74
22. Parlow J, Viale JP, Annat G, Hughson R, Quintin L (1995) Spontaneous cardiac baroreflex in humans. Comparison with drug-induced responsse. Hypertension 25:1058–1068
23. Pena MA, Echeverria JC, Garcia MT, Gonzalez-Camarena R (2009) Applying fractal analysis to short sets of heart rate variability data. Med Biol Eng Comput 47:709–17
24. Peng CK, Havlin S, Stanley HE, Goldberger AL (1995) Quantification of scaling exponents and crossover phenomena in nonstationary heartbeat time series. Chaos 5:82–87
25. Penzel T, Kantelhardt JW, Grote L, Peter JH, Bunde A (2003) Comparison of detrended fluctuation analysis and spectral analysis for heart rate variability in sleep and sleep apnea. IEEE Trans Biomed Eng 50:1143–51
26. Piskorski J, Guzik P (2005) Filtering Poincaré plots. Comput Meth Sci Technol 11:39–48
27. Piskorski J, Guzik P (2007) Geometry of the Poincaré plot of RR intervals and its asymmetry in healthy adults. Physiol Meas 28:287–300
28. Piskorski J, Guzik P (2011) Structure of heart rate asymmetry: deceleration and acceleration runs. Physiol Meas 32:1011–1023
29. Porta A, Casali KR, Casali AG, Gnecchi-Ruscone T, Tobaldini E, Montano N, Lange S, Geue D, Cysarz D, Van Leeuwen P (2008) Temporal asymmetries of short-term heart period variability are linked to autonomic regulation. Am J Physiol Regul Integr Comp Physiol 295:R550–R557
30. Porta A, D'addio G, Bassani T, Maestri R, Pinna GD (2009) Assessment of cardiovascular regulation through irreversibility analysis of heart period variability: a 24 hours Holter study in healthy and chronic heart failure populations. Phil Trans Royal Soc A 367:1359–1375
31. Rudas L, Crossman AA, Morillo CA, Halliwill JR, Tahvanainen KU, Kuusela TA, Eckberg DL (1999) Human sympathetic and vagal baroreflex responses to sequential nitroprusside and phenylephrine. Am J Physiol Heart Circ Physiol 276:H1691–H1698
32. Schneider R, Barthel P, Bauer A, Schmidt G (2004) libRASCH—a programming framework for signal handling. Comput Cardiol 31:53–56
33. Sears CE, Noble P, Noble D, Paterson DJ (1999) Vagal control of heart rate is modulated by extracellular potassium. J Auton Nerv Syst 77:164–1671
34. Task Force of the European Society of Cardiology and North American Society of Pacing and Electrophysiology (1996) Heart rate variability: standards of measurement, physiological interpretation, and clinical use. Circulation 93:1043–1065